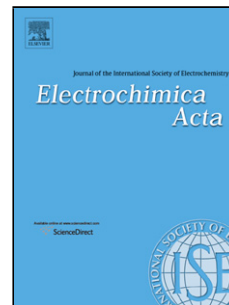


## Accepted Manuscript

Title: A Comparative Study of Nickel Electrodeposition Using Deep Eutectic Solvents and Aqueous Solutions

Author: Andrew P. Abbott Andrew Ballantyne Robert C. Harris Jamil A. Juma Karl S. Ryder



PII: S0013-4686(15)30118-3  
DOI: <http://dx.doi.org/doi:10.1016/j.electacta.2015.07.051>  
Reference: EA 25333

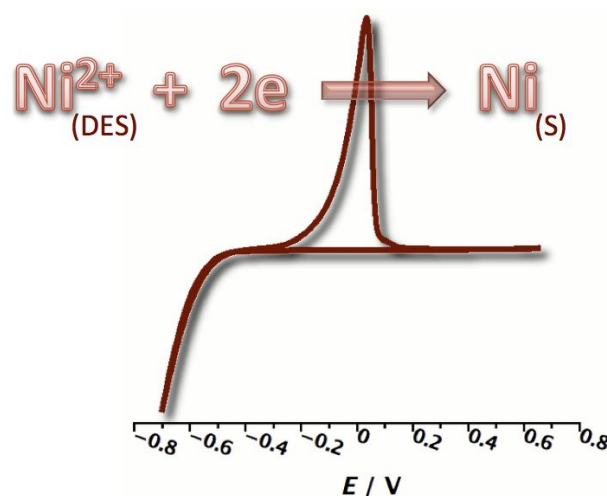
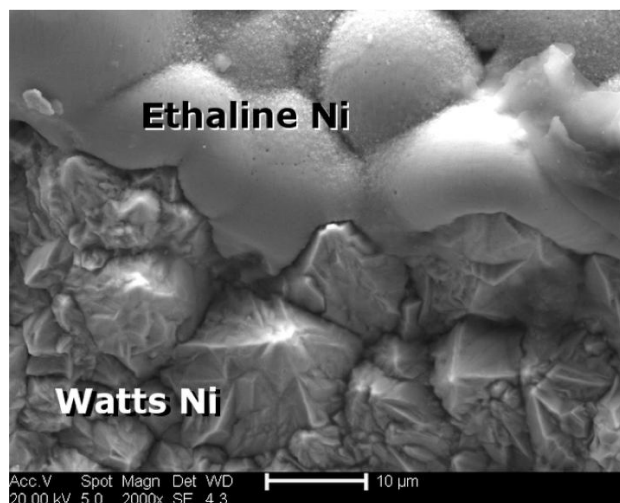
To appear in: *Electrochimica Acta*

Received date: 19-5-2015  
Revised date: 7-7-2015  
Accepted date: 9-7-2015

Please cite this article as: Andrew P.Abbott, Andrew Ballantyne, Robert C.Harris, Jamil A.Juma, Karl S.Ryder, A Comparative Study of Nickel Electrodeposition Using Deep Eutectic Solvents and Aqueous Solutions, *Electrochimica Acta* <http://dx.doi.org/10.1016/j.electacta.2015.07.051>

This is a PDF file of an unedited manuscript that has been accepted for publication. As a service to our customers we are providing this early version of the manuscript. The manuscript will undergo copyediting, typesetting, and review of the resulting proof before it is published in its final form. Please note that during the production process errors may be discovered which could affect the content, and all legal disclaimers that apply to the journal pertain.

## Graphical Abstract

**Highlights:**

- Facile electro-deposition of bright Ni is possible from DES electrolytes at elevated temp. and high concentration.
- Harder Ni deposits are obtained from DES than from aqueous electrolytes.
- Similar deposition rates are measured despite the higher viscosity of the DES.
- High temp. speciation of  $Ni^{2+}$  in DES determines morphology of deposit.
- Ni deposition in DES shows a levelling effect when compared to Ni plating in aqueous electrolytes.

## **A Comparative Study of Nickel Electrodeposition Using Deep Eutectic Solvents and Aqueous Solutions**

Andrew P. Abbott <sup>1</sup>, Andrew Ballantyne <sup>1</sup>, Robert C. Harris <sup>1</sup>, Jamil A. Juma <sup>1,2</sup>  
and Karl S. Ryder <sup>1</sup> \*

<sup>1</sup> Materials Centre, Department of Chemistry, University of Leicester, Leicester, UK LE1 7RH.

e-mail: k.s.ryder@le.ac.uk; Fax: (+44) (0)116 252 3789

<sup>2</sup> Chemistry Department, University of Koya, Arbil, Iraq

### **Abstract**

Metal electrodeposition using ionic liquid electrolytes and deep eutectic solvents is now well known but to our knowledge for electrolytic deposition of metals such as nickel no direct comparison has thus far been drawn between deposition using aqueous solutions and DES under otherwise identical conditions. In the current study it is shown that nickel deposition can be carried out with similar deposition rates in aqueous and ionic media despite the significant differences in viscosity and conductivity. It is, however, shown that in ionic media the morphology of the deposits is markedly different from that achieved using a Watts nickel bath and that one aspect of these differences manifests itself in significant increase in the coating hardness. It is proposed that the observed morphology differences occur due to the variations of nickel speciation in each electrolyte environment.

### **Key Words**

Electroplating, nickel, deep eutectic solvents, speciation.

## Introduction

Nickel electrodeposits are used extensively for corrosion resistance, decorative applications and in the fabrication of printed electronic circuitry.<sup>1-3</sup> Oliver P. Watts formulated a general purpose nickel bath composition in 1916 (nickel sulfate, nickel chloride, and boric acid)<sup>4</sup> that has since been widely used and adopted for commercial processes.<sup>5-7</sup> The Watts nickel bath has since been extensively applied and modified to produce a range of functional and decorative nickel finishes.<sup>8, 9</sup> The variation in coating morphology and other physical properties is achieved using a variety of organic and inorganic additives to brighten and level the nickel deposit.<sup>10, 11</sup> On the other hand the Watts bath has to be operated under close and attentive process control. Small variations in composition and pH can influence the deposit morphology, coating properties and adhesion.

In a general drive to overcome some of the drawbacks of electroplating in aqueous solutions (for example low current efficiency, stringent process control, complexity of bath and additives) the electrodeposition of metals using ionic liquids and deep eutectic solvents (DES) is a topic which is currently gaining significant attention due to the ability to deposit reactive metals and metal-alloys that are otherwise not attainable in aqueous solution and to access novel architectures. There are, however, fundamental differences between molecular solvent and ionic DES electrolytes and these undoubtedly change the way in which metals nucleate and grow on surfaces. In the context of our current work there have been several recent studies of the electrochemical deposition of nickel and nickel alloys (with for example Zn, Sn, Co or P) from DES.<sup>2, 12-17</sup> These studies have all uniquely focused on the electrochemical deposition of the metal or alloy system from a single electrolyte, DES, system. To our knowledge no work has been carried out to compare directly the properties of metals deposited from aqueous solutions with those from ionic liquids under exactly the same conditions of concentration and temperature.<sup>18-21</sup> As a result of such a comparative study we seek to understand the influence of the electrolyte on deposition rate, current efficiency and deposit morphology as well as metal ion speciation.

It has previously been shown that deep-eutectic solvents (DES), which are mixtures of quaternary ammonium salts with either hydrogen bond donors or metal salts, can be used for metal deposition.<sup>22</sup> One of the most effective of these DES electrolytes is a stoichiometric mix of ethylene glycol and choline chloride in a ratio of 2:1. This DES is known by the trivial (commercial) name of *Ethaline*. Electrodeposition of Zn, Cr, Ag, Ni, Zn-Sn alloys and Cu composites from Ethaline have been demonstrated.<sup>23</sup> The deposit morphology differs markedly

in most cases from that obtained during electrodeposition of the same metal in aqueous solutions and is significantly affected by the content (electrolyte formulation) and operating conditions of the process.<sup>24</sup> The nucleation and growth of metal coatings from solution depends clearly upon the physical conditions of temperature and applied potential and current but it also is strongly affected by metal speciation, mass transport and double layer properties. In this manuscript we describe a study of nickel electrodeposition from three comparable nickel solutions, these are;

- Watts nickel bath:  $1.14 \text{ mol dm}^{-3} \text{ NiSO}_4$ ,  $0.51 \text{ mol dm}^{-3} \text{ NaCl}$ ,  $0.65 \text{ mol dm}^{-3} \text{ B(OH)}_3$  in water.
- Aqueous solution:  $1.14 \text{ mol dm}^{-3} \text{ NiCl}_2 \cdot 6\text{H}_2\text{O}$  in water.
- Ethaline:  $1.14 \text{ mol dm}^{-3} \text{ NiCl}_2 \cdot 6\text{H}_2\text{O}$  in 1ChCl: 2 ethylene glycol

The effects of speciation and mass transport were studied while maintaining constant temperature, concentration and electrochemical control. Using the Watts nickel bath as a standard the operating conditions of  $1.14 \text{ mol dm}^{-3}$  and  $80 \text{ }^\circ\text{C}$  were used throughout the electrochemical experiments. This leaves the speciation, mass transport and double layer structure as the remaining significant variables between the systems.

## Experimental

Choline chloride,  $[\text{HOC}_2\text{H}_4\text{N}(\text{CH}_3)_3\text{Cl}]$  (ChCl) (Aldrich 99 %) was recrystallized from absolute ethanol, filtered and dried under vacuum. Ethylene glycol (EG) (Aldrich + 99 %), was used as received. The two components have been mixed together by stirring (in a 1: 2 molar ratio of ChCl: hydrogen bond donor) at  $60 \text{ }^\circ\text{C}$  until a homogeneous, colourless liquid formed. The nickel salts;  $\text{NiCl}_2 \cdot 6\text{H}_2\text{O}$  and  $\text{NiSO}_4 \cdot 6\text{H}_2\text{O}$  (Aldrich  $\geq 98 \%$ ), sodium chloride and boric acid (BDH Chemical, 99.8%) were used as purchased. The concentration of nickel salts in all liquids was  $1.14 \text{ mol dm}^{-3}$  (except where explicitly stated).

The conductivity of the liquids was measured as function of temperature using a Jenway 4510 conductivity meter fitted with an inherent temperature probe (cell constant =  $1.01 \text{ cm}^{-1}$ ). Cyclic voltammetry investigations were carried out using an Autolab PGSTAT12 potentiostat controlled with GPES2 software. A three-electrode system was used, consisting of a platinum working-electrode ( $0.12 \text{ cm}^2$  area), a platinum flag counter-electrode and a silver wire pseudo-reference electrode. The working electrode was polished with  $0.05 \text{ } \mu\text{m}$   $\gamma$ -alumina paste and cleaned by rinsing with deionised water followed by acetone prior to each experiment. All cyclic voltammograms were recorded at  $80 \text{ }^\circ\text{C}$  and at a scan rate of  $5\text{-}10 \text{ mV s}^{-1}$ . Quartz crystal microbalance (QCM) was used to determine current efficiency. An electrochemical quartz

crystal microbalance consisting of an Agilent HPE5061A network analyser with a 10 MHz AT-cut gold quartz crystal (International Crystal Manufacturing Co., Oklahoma City, USA) was used. A three-electrode compartment cell was constructed from PTFE, with a polished gold coated crystal working electrode, a silver wire reference electrode and a Pt flag counter electrode. The electrodes were connected to a potentiostat (Autolab 263A) in order to record voltammetric data. The quartz crystal had a piezoelectrically active area of  $0.23 \text{ cm}^2$ .

Bulk electrolysis was carried out using cathodic plates (nickel and mild steel,  $50 \text{ mm} \times 42 \text{ mm} \times 1 \text{ mm}$ ) which were mechanically polished and cleaned with acetone and rinsed with water and dried. An iridium oxide-coated titanium mesh electrode,  $40 \text{ mm} \times 50 \text{ mm}$ , was used as an anode. In all of the experiments the solution temperature was  $80 \text{ }^\circ\text{C}$  and deposition was carried out using a constant current for 3 to 9 hours, after which the substrates were removed from solution and washed with water and acetone.

Surface microstructure analysis: The surface morphology was characterised using scanning electron microscopy (SEM) and elemental analysis of the deposit compositions was carried out by energy dispersive X-ray spectroscopy (EDX), using a Phillips XL30 ESEM instrument with an accelerating voltage between 15 and 20 keV, giving an average beam current of *ca.*  $120 \text{ }\mu\text{A}$ .

Cross-section microstructure: The samples were mounted in a resin using a Struers Labo Press 3. The samples were then polished first with 240 grit silicon carbide paper to make them flat, then with diamond abrasives of successively  $9 \text{ }\mu\text{m}$  and  $3 \text{ }\mu\text{m}$  size and finally with  $0.5 \text{ }\mu\text{m}$  colloidal silicon carbide paste.

UV visible spectrophotometer: A Shimadzu model UV-1601 spectrophotometer was used with the cell path length equal to 10 mm. Values for  $\lambda_{\text{max}}$  were determined using the spectrophotometer's built-in peak-pick feature, using UV- probe software.

Hardness: The hardness of the electrodeposits was evaluated as resistance to indentation, in the form of force of indentation and depth of indentation, for nickel deposits on copper and nickel with a Mitutoyo model MVK-G100 hardness meter. The specimens were indented using different forces and a loading rate of  $0.1 \text{ mm s}^{-1}$  for 10 s. The Vickers number is the number obtained by dividing the kg-force load by the square area of indentation of a standard probe.

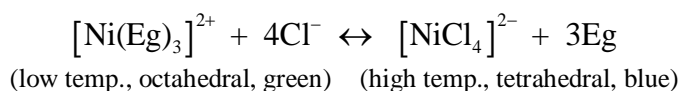
## Results and Discussion

Most studies of metal deposition in ionic liquids have been carried out at relatively low ( $10^{-3}$  molar) metal ion concentrations and at ambient temperatures. This is in stark contrast to the conditions commonly used for commercial metal electroplating in aqueous solutions which is generally performed at much higher concentration (molar) and higher temperatures. The

electrodeposition of Ni has previously been studied in Ethaline using  $0.2 \text{ mol dm}^{-3} \text{ NiCl}_2 \cdot 6\text{H}_2\text{O}$  at  $20 \text{ }^\circ\text{C}$ .<sup>24</sup> Black deposits were obtained from bulk deposition and metallic looking deposits could only be obtained using ethylene diamine as an additive.<sup>24</sup> The electrochemical behaviour previously reported showed a response which was poorly reversible with a large overpotential (*ca.*  $> 0.75 \text{ V}$ ) separating the deposition and stripping peaks in the voltammetry. In contrast to this **Figure 1** shows the cyclic voltammogram of a solution of  $\text{NiCl}_2 \cdot 6\text{H}_2\text{O}$  in Ethaline. In this case the concentration is increased to a  $1.14 \text{ mol dm}^{-3}$  which is the same as that used for  $[\text{Ni}^{2+}]$  ion in the aqueous Watts nickel bath. At this higher concentration of  $\text{Ni}^{2+}$  a more reversible redox behaviour is observed in Ethaline than that previously reported and a clear nucleation loop can be observed at  $-0.5 \text{ V}$ . Despite the improved electrochemical response evidenced in **Figure 1**, (compared to that shown in reference 24) bulk deposition at room temperature from  $1.14 \text{ mol dm}^{-3} \text{ NiCl}_2 \cdot 6\text{H}_2\text{O}$  in Ethaline at  $25 \text{ }^\circ\text{C}$  leads to a patchy, dull and friable nickel deposit as can be seen from **Figure 2**.

**Speciation:** Commercial aqueous nickel plating solutions are generally operated at elevated temperatures (*e.g.*  $80 \text{ }^\circ\text{C}$ ), this clearly increases conductivity and decreases viscosity of the electrolyte but it can also affect the metal ion speciation. This effect is especially relevant to nickel electrochemistry as ligand exchange processes for  $\text{Ni}^{2+}$  in aqueous solution are known to be very slow at room temperature. In addition, solution colour is a good indication of metal ion speciation and many metal salts are known to show significant thermochromism in DES electrolytes. Thermochromism is the reversible property of substances to change colour due to a change in temperature.<sup>25</sup> Thermochromism of a range of transition metal complexes both in conventional ionic liquids and in DES media has been reported.<sup>26-28</sup> In DES media it has been previously reported that only  $\text{NiCl}_2 \cdot 6\text{H}_2\text{O}$  displayed significant, stable, behaviour.<sup>27, 28</sup> The thermochromic behaviour of a solution of  $\text{NiCl}_2 \cdot 6\text{H}_2\text{O}$  in Ethaline studied here is shown graphically in **Figure 3**. The temperature dependant UV-Vis spectra of the  $\text{Ni}^{2+}$  ion in Ethaline, **Figure 3a**, along with the associated colour changes, **Figure 3b**, agree closely with the previous study.<sup>28</sup> The low temperature spectra show two sets of absorption bands centred on  $425 \text{ nm}$ , band I, and  $655\text{--}715 \text{ nm}$ , band II. The absorptions at band I are attributed to the  ${}^3\text{A}_{2g}(\text{F}) \rightarrow {}^3\text{T}_{1g}(\text{P})$  transition of the octahedral  $\text{Ni}^{2+}$  ion.<sup>28</sup> In aqueous solution this is commonly  $[\text{Ni}(\text{H}_2\text{O})_6]^{2+}$ , however, we have recently reported that in Ethaline the  $\text{Ni}^{2+}$  species can be attributed to the ethylene glycol (Eg) complex  $[\text{Ni}(\text{Eg})_3]^{2+}$ .<sup>29</sup> This band does not show a strong temperature dependence although the intensity does decrease with increasing temperature. The absorptions in band II show a strong temperature dependence. There is a shift to lower

wavelength with increasing temperature and there are additional bands appearing at lower wavelength around 600 nm. This is consistent with the previous observations<sup>28</sup> and the increasing intensity of the lower wavelength bands with increasing temperature is attributed to the  ${}^3T_1(F) \rightarrow {}^3T_1(P)$  transition of the tetrahedral  $[\text{NiCl}_4]^{2-}$  species.<sup>28</sup> This corresponds to the colour change from pale green (at low temp.) to blue (at high temp.). The thermochromic process is represented below.



An important observation here is that effective electroplating and facile voltammetry occurs only at higher temperatures where the tetrahedral anion is dominant. This is discussed later.

**Figure 4** shows the UV-vis spectra of the three  $\text{Ni}^{2+}$  solutions as well as their visible appearance at room temperature. At the same concentration of  $\text{Ni}^{2+}$  the solutions are different shades of green and have different intensities indicating some variance of speciation. The spectra for all three are similar and consistent with the presence of the octahedral species in each bath. The spectrum for the  $\text{NiCl}_2(6\text{H}_2\text{O})$  aqueous solution and the Watts bath are also similar, however, the Watts spectrum does not show the band at short wavelength around 260 nm. The Watts bath is made by dissolution of  $\text{NiSO}_4$  in water with following addition of  $\text{HCl}$  and other minor components. In this case it is unlikely that chloride would displace water in the coordination sphere on the basis of mass action, thus the dominant species would be  $[\text{Ni}(\text{H}_2\text{O})_6]^{2+}$ . Studies have shown that water can be displaced by chloride at room temperature in aqueous solution but that much higher concentrations of chloride are required.<sup>30</sup> On the other hand where the aqueous solution of  $\text{NiCl}_2(6\text{H}_2\text{O})$  is made up from dissolution of the salt, chloride will persist in the coordination sphere because the ligand exchange kinetics for  $\text{Ni}^{2+}$  are slow at room temperature. Under these conditions the dominant species may be  $[\text{NiCl}_2(\text{H}_2\text{O})_4]$ . Consequently the spectral differences may be accounted for by the presence of either  $[\text{Ni}(\text{H}_2\text{O})_6]^{2+}$  or  $[\text{NiCl}_2(\text{H}_2\text{O})_4]$ . In the case of the Ethaline solution the increased intensity of the peaks, band I and II, reflect the presence of glycol in the coordination sphere rather than water. The band at 260 nm is much smaller in relative terms than either the aqueous solution of  $\text{NiCl}_2(6\text{H}_2\text{O})$  or the Watts bath and may represent the presence of some of the chloride bound species in equilibrium with the glycol species.

**Physical Properties, DES:** DESs and ionic liquids are well known to be considerably more viscous than aqueous solutions. The viscosity of the  $\text{Ni}^{2+}$  solution ( $1.14 \text{ mol dm}^{-3}$ ) in Ethaline, Watts bath and water were found to be 16.80 , 0.838 and 0.693 cP at  $80 \text{ }^\circ\text{C}$  respectively. The higher viscosity clearly slows down mass transport and decreases conductivity in solution. It is often assumed that this makes metal deposition slow in ionic liquids. **Figure 5** shows the conductivity of the different systems as a function of temperature and as expected the DES has by far the lowest conductivity. With slower mass transport and lower conductivity it might be expected that the comparable nickel ion reduction current in Ethaline might be smaller in magnitude than that in either of the aqueous solutions. **Figure 6** shows the cyclic voltammetry for the solutions at the same concentration and temperature. The most striking feature here, compared with **Figure 1** at room temperature, is that the magnitude of peak currents is much higher as a consequence of improved conductivity and viscosity. Additionally the wave shapes at higher temperature indicate faster electrochemical kinetics that we attribute to the presence of the  $[\text{NiCl}_4]^{2-}$  anion.

For clarity of interpretation the potential data in **Figure 6a** have been referenced to the  $[\text{Fe}(\text{CN})_6]^{3-/4-}$  couple which has been shown to be a reliable reference in these two liquids. The onset potential for nickel ion reduction is similar in all three solutions. The reduction current in Ethaline is larger and the stripping charge is also larger than the two aqueous solutions despite the decreased conductivity and increased viscosity of the former. This suggests that mass transport is not the dominant factor controlling the nickel deposition rate. This is an important result as it shows that metal deposition from ionic liquids / DES does not necessarily have to be slower than that from aqueous solutions under equivalent conditions.

The nickel reduction and deposition processes have been previously studied in Ethaline at room temperature.<sup>24</sup> It was shown that the process was only quasi-reversible and needed a strong ligand such as ethylene diamine to strip the nickel effectively from the electrode surface. Here we have shown that the difference between the reduction potential and the re-oxidation potential is smaller in magnitude at higher temperature and with increased concentration. The observation that the reductive and oxidative currents for the 3 liquids, **Figure 6a**, do not scale with the conductivity or viscosity suggests that mass transport is not the only factor affecting the rate of nickel growth.

**Figure 6b** also shows the voltammetry of the Ethaline system as a function of nickel chloride concentration at a fixed potential scan rate of  $10\text{mV s}^{-1}$ . One striking feature of this data set is that it is clear that higher temperature, even at relatively low concentration, is favourable for facile Ni deposition and stripping in the Ethaline electrolyte. Integration of the voltammograms reveals that in each case the deposition charge is approximately equal to the stripping charge. For example in a typical voltammogram at a  $\text{Ni}^{2+}$  concentration of  $0.9\text{ M}$  the deposition charge,  $Q_{\text{Dep}}$ , was determined as  $10\text{ mC}$  and the corresponding anodic stripping charge,  $Q_{\text{Strip}}$ , was measured as  $11\text{mC}$ . Further, the deposition charge,  $Q_{\text{Dep}}$ , is proportional the concentration of nickel. For example at  $[\text{Ni}^{2+}]$  of  $0.1\text{ M}$ ,  $Q_{\text{Dep}}$ , was determined as  $1.0\text{ mC}$ , where  $[\text{Ni}^{2+}]$  was increased to  $0.5\text{ M}$  corresponding  $Q_{\text{Dep}}$  was measured as  $6.0\text{ mC}$  and further increase of  $[\text{Ni}^{2+}]$   $0.9\text{ M}$  gave a  $Q_{\text{Dep}}$  of  $10\text{ mC}$ .

In all solutions the metal is present at high concentrations so it is not surprising that the deposition is not under diffusion control on the time scale of the voltammogram. It is more likely that migration controls mass transport and this will be concentration dependent. Potentiostatic electrodeposition experiments monitored using chronocoulometry were used to explore this observation. **Figure 7** shows comparable plots of charge vs square root of time for the deposition processes. These plots should be approximately linear for a diffusion controlled processes. However, this analysis is only valid if the current efficiency is high such that most of the current is consumed in metal deposition. The current efficiency for electrodeposition in the three electrolyte systems was determined separately using quartz crystal microbalance methods. Using an over-potential of  $-400\text{ mV}$  it was found that the current efficiency in all three liquids was between  $95$  and  $98\%$ . Consequently **Figure 7** shows that the rate of deposition is relatively similar in all three liquids when deposited at constant potential.

**Deposit properties:** The images presented in **Figure 8** show the morphology of the nickel layer deposited at constant current density (and for the same time) from the three liquids in both plan view and cross section. From the latter it can be seen that the deposit thickness is roughly the same in all three systems. It is clear that the nickel layer deposited from Ethaline is uniformly dense and results in a flat, featureless, surface which is mirror bright. The Watts nickel and deionised water solutions also gave dense deposits but the surface was rougher in both cases and this resulted in a dull, matt appearance.

The data presented in **Figure 9a** show the Vickers hardness of the Ni films obtained from each of nickel ion solutions. Each hardness measurement was determined from the average of  $5$  indentations made over a representative area of the coating. The deposit obtained from Ethaline

is considerably harder than that obtained in either of the two aqueous solutions. The Ni layer deposited from Ethaline demonstrates a constant hardness of 460 HV between 50 and 300 gf. This is considerably harder than the deposits obtained from aqueous nickel sulphate solutions at least matches the aqueous hard nickel values achieved using additives such ammonium chloride (*c.a.* 380-480 HV).<sup>31</sup>

**Figure 9b** shows the linear correlation between indentation depth and applied load for the hardness test. It has previously been reported that the hardness of nickel is related to the grain size which means that a nanocrystalline deposit is harder than microcrystalline nickel.<sup>32</sup> While the grain size cannot be determined from the cross-sectional images it is clear from the surface morphology that the deposits obtained from the aqueous solutions are more microcrystalline than those obtained from Ethaline.

**Effect of substrate:** Nickel is often applied as a decorative or protective coating to substrates such as mild steel, die-cast zinc or aluminium alloy components. It can be applied as a variety of duplex and triplex films, most notably with chromium to provide hard wearing surfaces.<sup>33</sup> The adhesion between the film and substrate is an essential feature for the coating. Inadequate or incorrect pre-treatment of the base metal substrate surface may lead to a lack of adhesion. *In situ* anodic etching is often used as a means of preparing the substrate for deposition by either roughening or de-passivating the surface. However, this can be detrimental to the ionic liquid electrolyte due to accumulation of substrate metal ions. This is often the case for various grades of stainless steel. Here the build-up of  $\text{Fe}^{3+}$  or  $\text{Fe}^{2+}$  in the electrolyte affects both the electrochemical and physical properties of the liquid and hence the quality of the coatings obtained. In such a case the anodic etch pre-treatment would have to take place in a separate liquid from that used for the bulk deposition.<sup>34</sup>

**Figure 10** shows the deposition of Ni on a mild steel substrate which has been etched *in-situ* by driving a current density of  $1 \text{ A dm}^{-2}$  for 30 sec. While adhesion is good under these conditions it is dependent upon current density and time and flaking and peeling can occur in all three plating solutions depending upon the pre-treatment conditions. This could be due to either weak bonding across the interfacial region or high stress because chloride increases the internal stress of the deposit. In addition chlorides tend to refine the grain size and minimize formation of nodules and trees which can aid adhesion.<sup>5</sup> **Figure 11** shows the electron micrograph of a layer deposited using the Watts nickel bath followed by a nickel layer deposited from Ethaline. Pyramidal growths are clearly formed in the Watts solution on the steel substrate which has been

etched by hydrochloric acid 35% then rinsed with deionization water and dried with acetone. In the case of  $\text{Ni}^{2+}$  in Ethaline bath a bright deposit entirely covers the rough surface from the deposit from the Watts bath. This shows that the Ethaline liquid is naturally levelling covering almost all of the pyramidal structures deposited from the aqueous solution. The microhardness depends to some magnitude on the test load applied also the deposit must be thick enough to sustain the measurement or the measurement must be conducted on a thick enough cross section in order to avoid substrate effects. Here the hardness of both Nickel layers were measured separately in cross section where the thickness of each layer was c.a. 110  $\mu\text{m}$  (shown in cross section **Figure 11**) and the applied load was 250 gf. The hardness of the Watts Ni layer was measured as 388 HV whereas that of the Ni layer deposited from Ethaline was 420 HV. Consequently a significant improvement in hardness of the Ni deposit was achieved.

Finally, it also seems likely that for any given substrate surface the formulation of the electrolyte will have an influence on the mechanisms of nucleation and growth of the Ni coatings. We have observed in previous studies of the electrodeposition of silver in DES electrolytes using *in-situ* holographic imaging and chronoamperometric methods that the mechanism of nucleation and growth is strongly dependant on the formulation of the DES. Changing the hydrogen bond donor component of the DES from ethylene glycol to urea results in a marked change in nucleation mechanism from progressive to instantaneous.<sup>35</sup> In the study presented here, qualitative analysis of the current time data (for which the integrated Cottrell plots are presented in **Figure 7**) shows that the rising portion of the  $i(t)$  curve, corresponding to nucleation and subsequent growth, is slower to develop in the Ethaline than in either of the aqueous electrolytes consistent with the voltammograms shown in **Figure 6**. Discussion of these data is beyond the scope of this manuscript but a quantitative mechanistic analysis of chronoamperometric data together with a study using RDE methods is the subject of an on-going investigation the results of which will be presented in a separate manuscript.

## Conclusions

This study has shown that under the same conditions of concentration and temperature nickel can be electrodeposited at comparable rates from a deep eutectic solvent and two aqueous solutions. This shows that the viscosity and conductivity are not the rate limiting factors for metal deposition. This study has shown that speciation is very different in the two liquids and this leads to different deposit morphologies. The ionic nickel plating liquid produces a morphology which is nano-crystalline whereas the two aqueous solutions produced micro-

crystalline deposits. The nickel deposit from DES has a considerably lower surface roughness and a mirror-bright surface finish whereas the two aqueous solutions are rough and matt in appearance. The nickel deposit from DES has a hardness value which is more than 100 HV harder than Watts nickel showing that the film has different mechanical properties than conventional nickel plate.

### **Acknowledgements**

The financial support of Ministry of higher education and scientific research in Kurdistan, Iraq, HCDP program is gratefully acknowledged for the studentship to JAJ. Also the authors acknowledge the financial support of the TSB (UK) under the RECONIF project (BA011K) and of the EU under Framework 7 for project CoLaBATS (FP7-ENV-2013 603482).

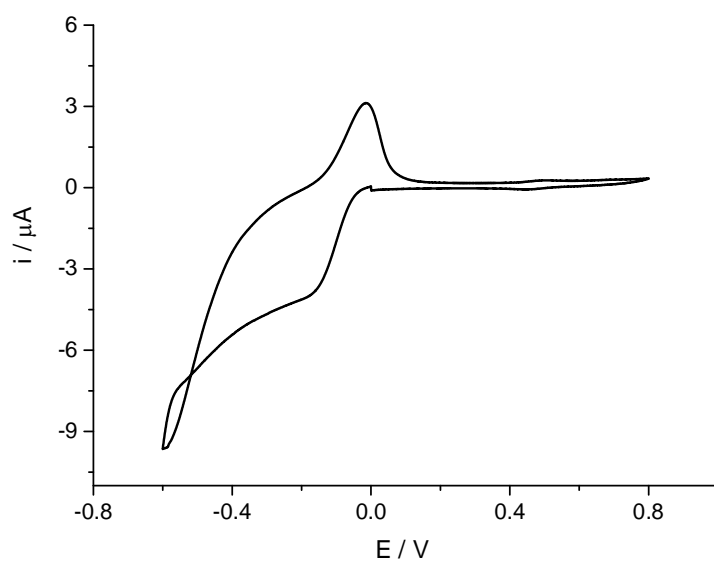
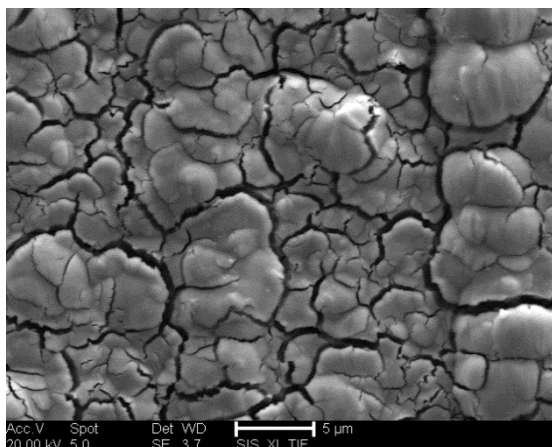


**Figure 1:** Cyclic voltammogram of  $1.14 \text{ mol dm}^{-3} \text{ NiCl}_2 \cdot 6\text{H}_2\text{O}$  in Ethaline at  $25 \text{ }^\circ\text{C}$  on a Pt electrode (1 mm disk), at a sweep rate of  $10 \text{ mV s}^{-1}$  vs  $[\text{Fe}(\text{CN})_6]^{4+/3+}$ .

a)



b)



**Figure 2:** Scanning electron micrograph (*left*) with a corresponding photo image (*right*) of the nickel coating resulting from electrodeposition at a driven current density of  $1.5 \text{ A dm}^{-3}$  for 1 hour in a  $1.14 \text{ mol dm}^{-3}$  solution of  $\text{NiCl}_2 \cdot 6\text{H}_2\text{O}$  in Ethaline at  $25 \text{ }^\circ\text{C}$ .

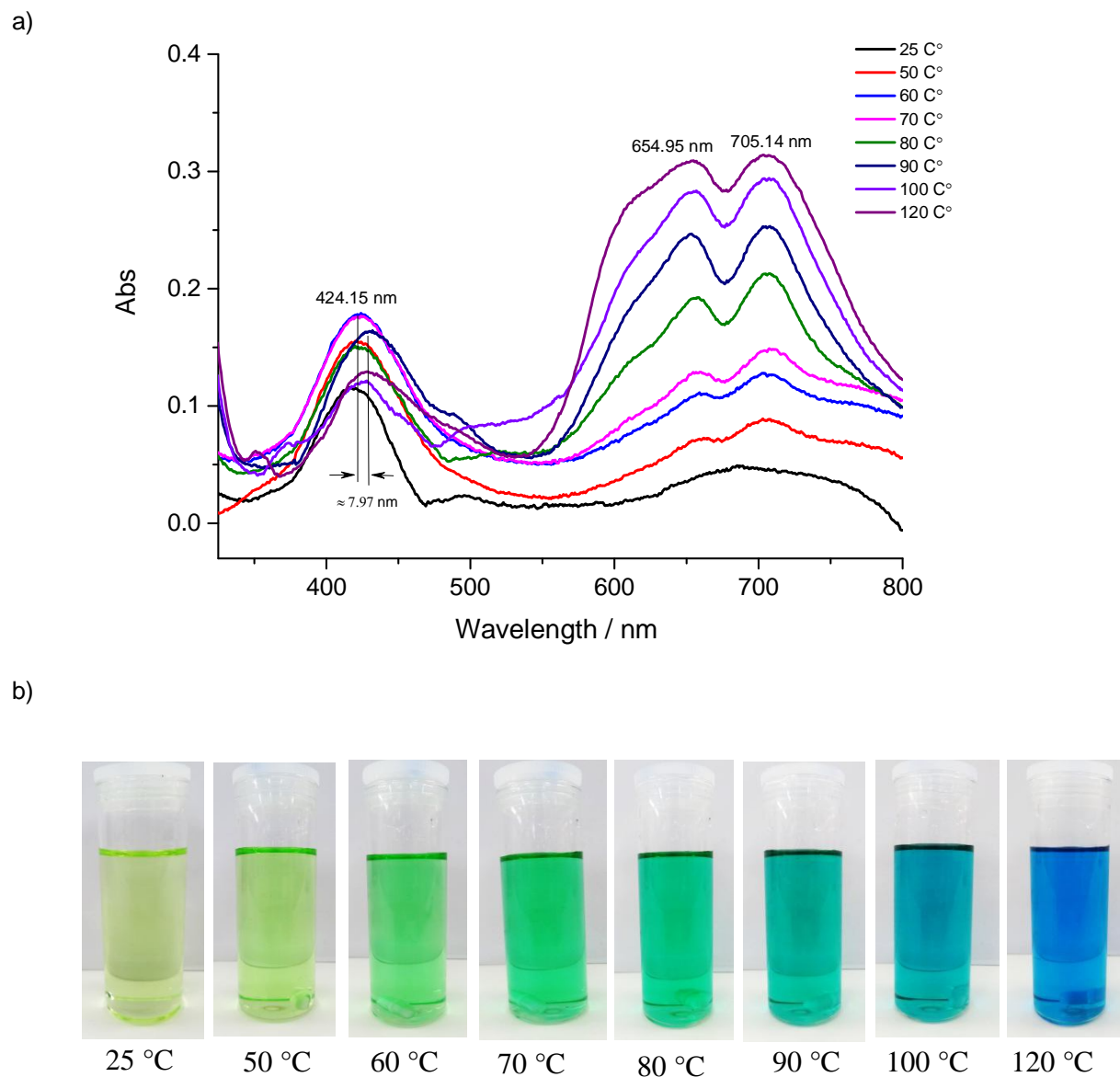


**Figure 3 :** a) UV-visible spectra of a  $0.02 \text{ mol dm}^{-3}$  solution of  $\text{NiCl}_2 \cdot 6\text{H}_2\text{O}$  in Ethaline measured over range of temperatures 25 – 120 °C; b) Photographic images of the same solution showing the temperature dependant colour changes.

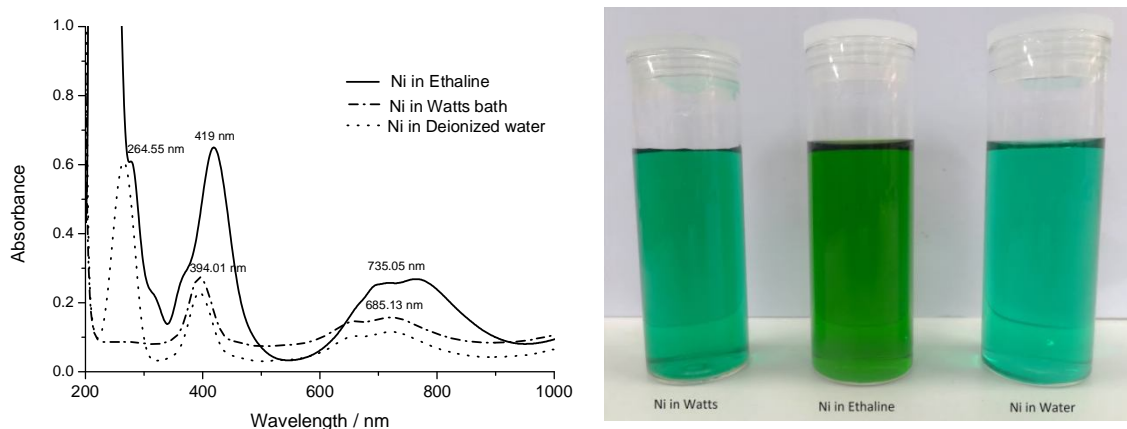


**Figure 4:** UV-Vis spectra (*left*) for  $\text{NiCl}_2 \cdot 6\text{H}_2\text{O}$  in different bath systems at room temp. and photograph of the nickel solutions at the same concentration ( $1.14 \text{ mol dm}^{-3}$ ) (*right*).

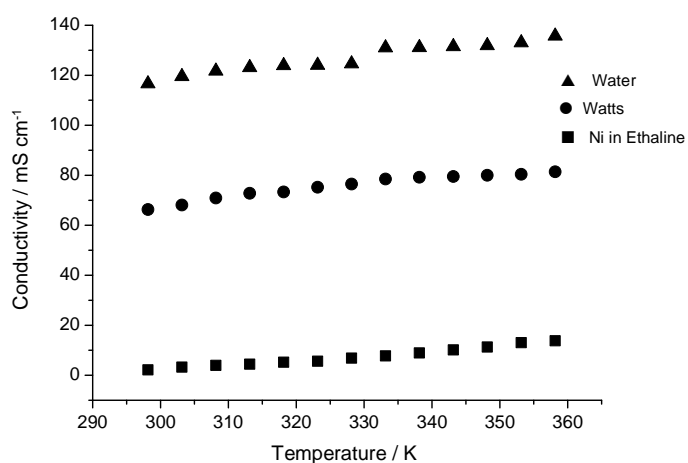


**Figure 5:** Conductivity of three different nickel plating systems (Watts bath, deionized water and Ethaline,  $[\text{Ni}^{2+}] 1.14 \text{ mol dm}^{-3}$ ) as a function of temperature.

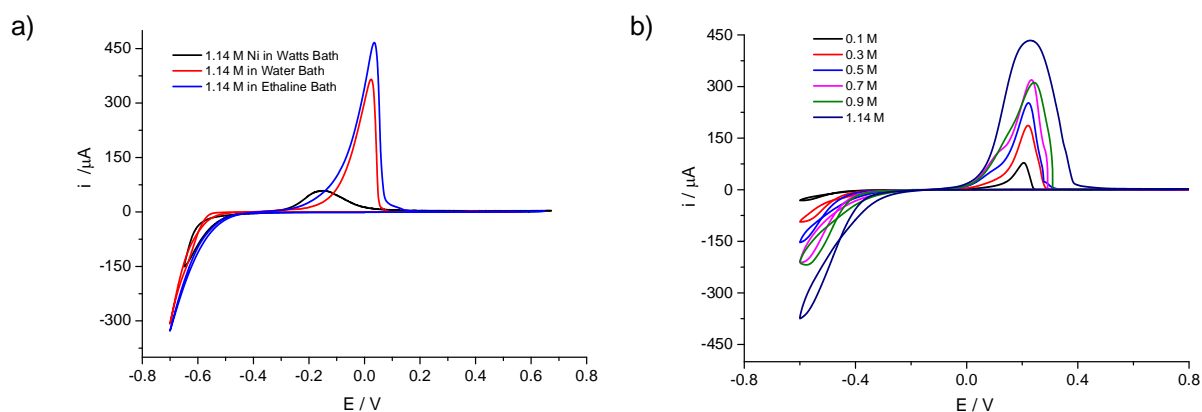


**Figure 6:** a) Cyclic voltammogram for 3 nickel containing systems at 80 °C at a sweep rate of 10 mV s<sup>-1</sup>; b) Cyclic voltammogram of [NiCl<sub>2</sub>·6H<sub>2</sub>O] in Ethaline as a function of concentration at sweep rate 5 mV s<sup>-1</sup> (all potentials *versus* [Fe(CN)<sub>6</sub>]<sup>4+/3+</sup> couple). CV data recorded at a Pt disc (1.0 mm diameter) electrode.

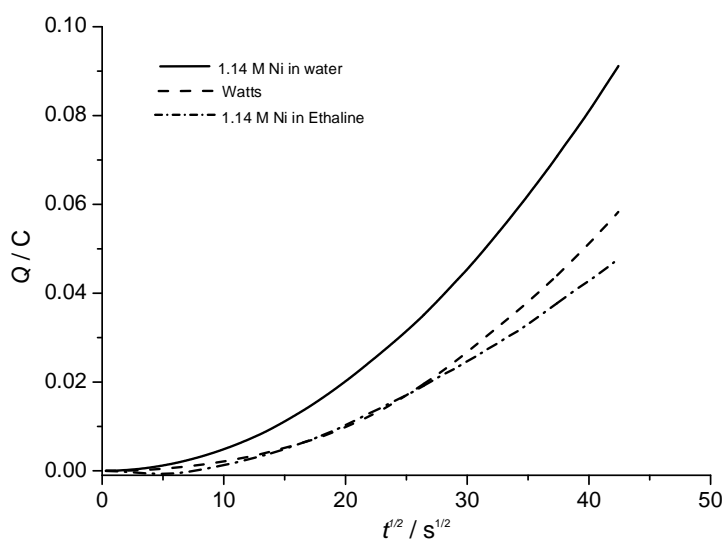


**Figure 7:** Chronocoulometry of Ni deposition for the three Ni<sup>2+</sup> solutions shown in **Figure 6a** at a 1 mm Pt disk. Deposition was carried out using a double potential step from OCP to +1.00 V (*versus* [Fe(CN)<sub>6</sub>]<sup>4+/3+</sup>) for 10s followed by a step to -1.00V for the remaining time (ca. 1600 s).

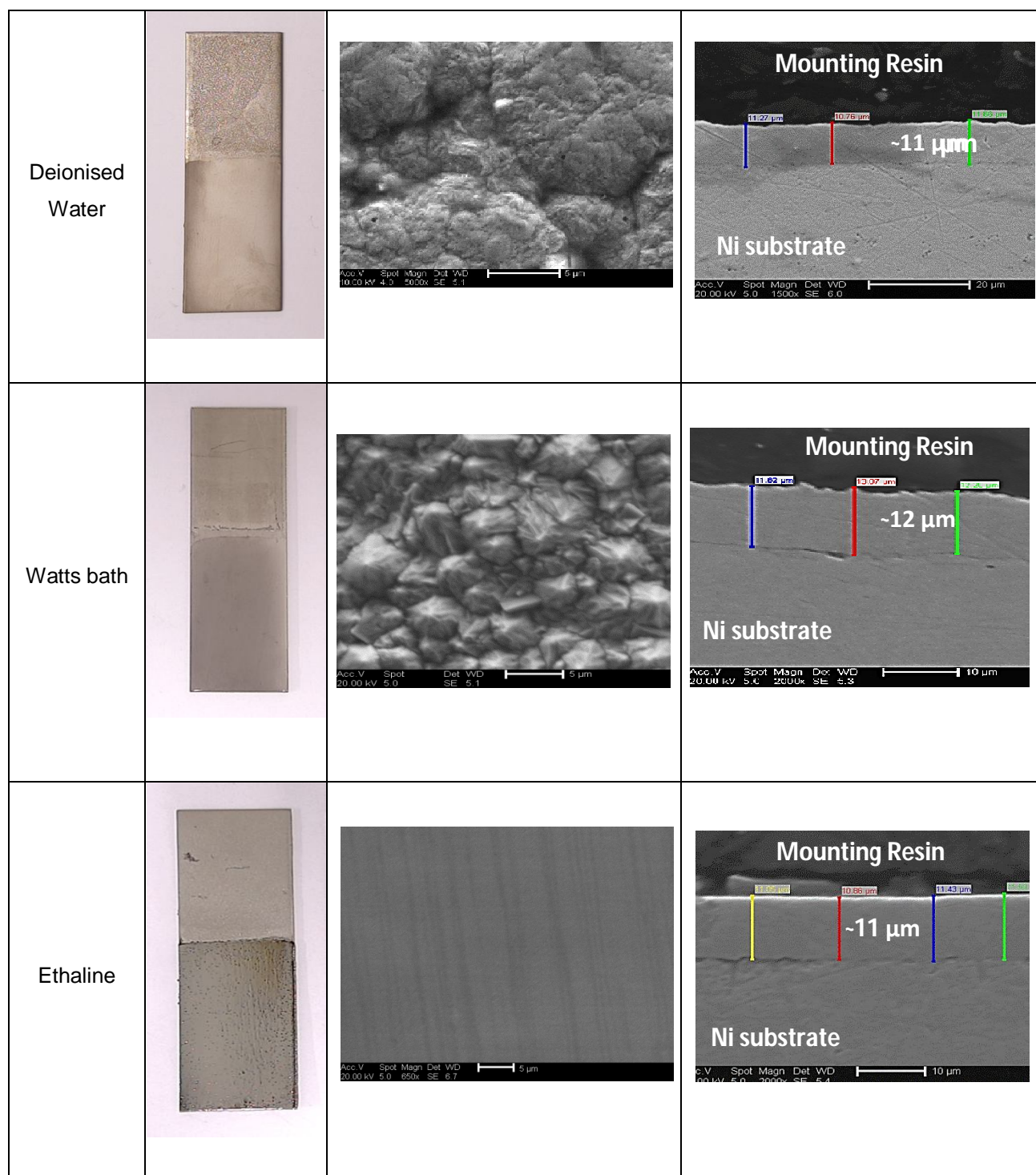


**Figure 8:** Scanning electron micrographs with cross sections showing samples after bulk electrodeposition from three different systems,  $1.14 \text{ mol dm}^{-3} \text{ NiCl}_2 \cdot 6\text{H}_2\text{O}$  in both deionized water and Ethaline and Watts bath (all at  $80^\circ \text{C}$  for 1 h on a nickel electrode at a driven current density of  $1.5 \text{ A dm}^{-3}$ ).

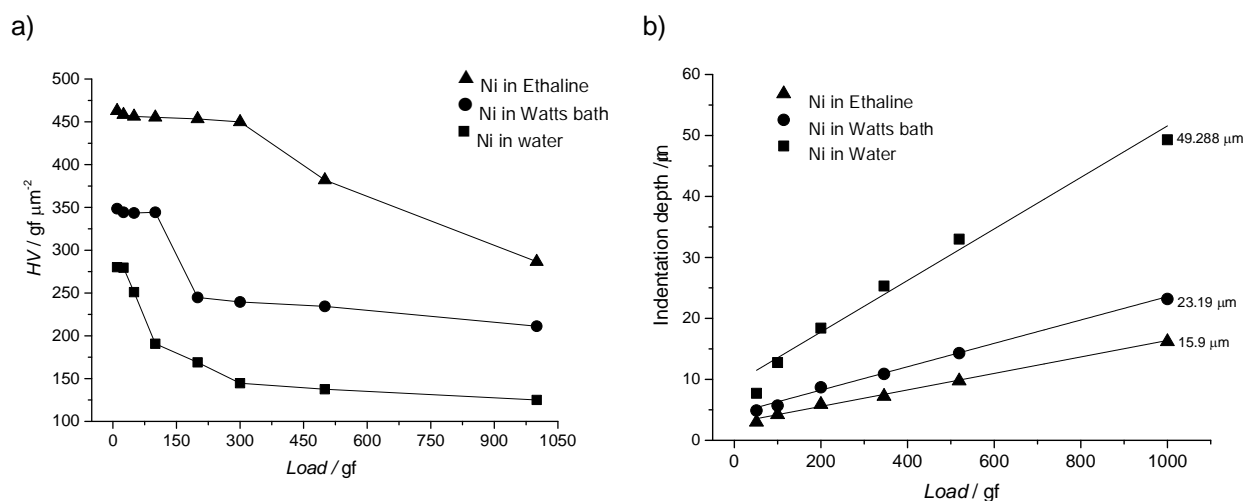


**Figure 9:** a) Vickers hardness of the nickel layers from different bath systems as a function of loading force; b) Indentation depth as a function of load for the nickel layer deposition from different systems. In each case the Ni coating thickness was measured as  $100 \mu\text{m}$ .



**Figure 10:** Photograph of a nickel layer deposited onto a mild steel substrate following electrolysis of  $\text{ChCl: 2 EG}$  containing  $1.14 \text{ mol dm}^{-3}$  at  $80 \text{ }^\circ\text{C}$  and current density of  $1.5 \text{ A dm}^{-3}$  for 1 h. The substrate was etched in-situ by applying  $1 \text{ A dm}^{-2}$  for 30 sec.

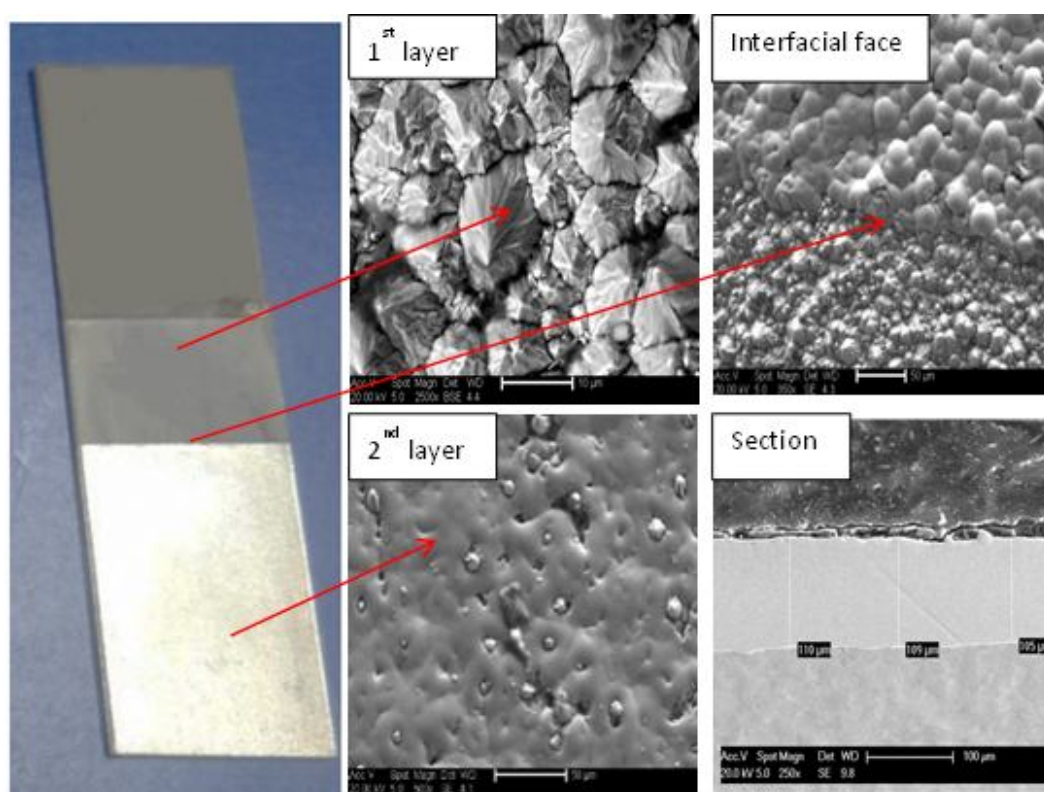


**Figure 11:** SEM micrographs and cross-sections of bulk electrodeposition of the duplex nickel coating from two different bath systems: 1<sup>st</sup> layer microstructured-Ni from a Watts bath at 60 °C with a driven current density of 2.5 A dm<sup>-3</sup> and the 2<sup>nd</sup> layer nanostructured-Ni from 1.14 mol dm<sup>-3</sup> NiCl<sub>2</sub>·6H<sub>2</sub>O in Ethaline at a driven current density of 0.33 A dm<sup>-3</sup> both system for 3 h on a mild steel electrode.

## References:

1. J. K. Dennis and T. E. Such, *Nickel and Chromium Plating*, Elsevier Science 2013.
2. M. R. Ali., M. d. Z. Rahman. and S. Saha., *Indian Journal of Chemical Technology*, 2014, **21**, 127-133.
3. H. Yang, X. Guo, N. Birbilis, G. Wu and W. Ding, *Applied Surface Science*, 2011, **257**, 9094-9102.
4. O. Watts, *Transactions of the American Electrochemical Society*, 1916, **29**, 395.
5. M. P. Mordechay Schlesinger, *Modern Electroplating* 2010.
6. D. Grujicic and B. Pesic, *Electrochim Acta*, 2006, **51**, 2678-2690.
7. J. P. Hoare, *Journal of The Electrochemical Society*, 1986, **133**, 2491.
8. E. M. Oliveira, G. A. Finazzi and I. A. Carlos, *Surface and Coatings Technology*, 2006, **200**, 5978-5985.
9. M. Supicova, R. Rozik, L. Trnkova, R. Orinakova and M. Galova, *Journal of Solid State Electrochemistry*, 2006, **10**, 61-68.
10. T. Mimani. and S. M. Mayanna., *J Appl Electrochem*, 1993, **23**, 339-345.
11. R. Well. and H. C. Cook., *Journal of the Electrochemical Society*, 1962, **109**, 295-301.
12. C. Gu and J. Tu, *Langmuir : the ACS journal of surfaces and colloids*, 2011, **27**, 10132-10140.
13. Y. You, C. Gu, X. Wang and J. Tu, *Journal of the Electrochemical Society*, 2012, **159**, D642-D648.
14. Y. H. You., C. D. Gu., X. L. Wang. and J. P. Tu., *Surf Coat Tech*, 2012, **206**, 3632-3638.
15. J. Vijayakumar, S. Mohan, S. Anand Kumar, S. R. Suseendiran and S. Pavithra, *International Journal of Hydrogen Energy*, 2013, **38**, 10208-10214.
16. L. Anicai, A. Petica, S. Costovici, P. Prioteasa and T. Visan, *Electrochim Acta*, 2013, **114**, 868-877.
17. S. Fashu, C. D. Gu, X. L. Wang and J. P. Tu, *Surface and Coatings Technology*, 2014, **242**, 34-41.
18. A. P. Abbott and K. J. McKenzie, *Physical Chemistry Chemical Physics*, 2006, **8**, 4265-4279.
19. Q. Zhang, K. De Oliveira Vigier, S. Royer and F. Jerome, *Chemical Society reviews*, 2012, **41**, 7108-7146.
20. A. P. Abbott, G. Capper, D. L. Davies and R. Rasheed, *Inorganic Chemistry*, 2004, **43**, 3447-3452.
21. J. S. Wilkes, *ACS Symp. Ser.*, 2002, **818**, 214.
22. A. P. Abbott, G. Capper, D. L. Davies, R. K. Rasheed and V. Tambyrajah, *Chemical Communications*, 2003, 70-71.
23. E. L. Smith, J. C. Barron, A. P. Abbott and K. S. Ryder, *Analytical Chemistry*, 2009, **81**, 8466-8471.
24. A. P. Abbott, K. El Ttaib, K. S. Ryder and E. L. Smith, *Transaction of the Institute Metal Finishing*, 2008, **86**, 234-240.
25. W. Linert, Y. Fukuda and A. Camard, *Coordination Chemistry Reviews*, 2001, **218**, 113-152.
26. X. Wei, L. Yu, D. Wang, X. Jin and G. Z. Chen, *Green Chem*, 2008, **10**, 296.
27. E. L. Smith, A. P. Abbott and K. S. Ryder, *Chemical reviews*, 2014, **114**, 11060-11082.
28. C.-D. Gu and J.-P. Tu, *RSC Advances*, 2011, **1**, 1220.
29. J. M. Hartley, C. M. Ip, G. C. Forrest, K. Singh, S. J. Gurman, K. S. Ryder, A. P. Abbott and G. Frisch, *Inorg Chem*, 2014, **53**, 6280-6288.
30. W. Liu, A. Migdisov and A. Williams-Jones, *Geochimica et Cosmochimica Acta*, 2012, **94**, 276-290.
31. W. A. Wesley. and E. J. Roehl., *Journal of Electrochemical Society*, 1942, **82**, 37-53.
32. K. E. ttaib, Doctor of Philosophy, University of Leicester, 2010.
33. J. K. Dennis and T. E. Such, *Nickel and Chromium Plating*, Elsevier Science 1993.
34. F. Endres, D. MacFarlane and A. Abbott, *Electrodeposition from Ionic Liquids*, Wiley 2008.
35. A. P. Abbott, M. Azam, K. S. Ryder and S. Saleem, *Anal Chem*, 2013, **85**, 6653-6660.